Supplementary Methods

Determination of Telomerase Activity

The TeloTAGGG Telomerase PCR Elisa (Roche), a photometric enzyme immunoassay that utilises the telomeric repeat amplification (TRAP) assay for the detection of telomerase activity was utilised according to manufacturers instructions.

Incucyte Growth and Apoptosis Assays

For assessment of growth and apoptosis following *ATRX* deletion according to p53 status, the *TP53* wild type SKNSH cell line and *TP53* mutant clone p53(2) were transfected with the *ATRX* CRISPR Cas9 construct then incubated overnight. The following morning 2000 RFP-Paprika expressing cells were FACS sorted into each well of a 96 well plate, in triplicate for each indication. The Incucyte Annexin V green reagent (Essen Bioscience) was then added to each well at a concentration of 1:200, then the plate was placed in the IncuCyte® live cell analysis system. Growth was assessed by serial phase microscopy images and apoptosis by quantification of the green fluorescent signal in serial images.

Whole genome sequencing

Copy number plots, LST (large scale transition) score, TAI (telomeric allelic imbalance) score and LOH (loss of heterozygosity) scores were obtained running ACESeq no control workflow (1) version 5.0.1-0, which is available from https://github.com/DKFZ-ODCF/ACEseqWorkflow. In short, the LST score is based on the number of breakpoint between regions ranging from 3-10 mb. The LOH score estimates the number of LOH regions, which are longer than 15 mb. Calculation of LOH and LST was done in principle as described by Popova et al (2). TAI score was used as an estimate of the number regions showing allelic imbalance towards the subtelomere, but not crossing the centromere. TAI calculation was done based on unmerged segments. HRD scores were calculated as sum of the LOH score, TAI score and LST score. For the indel calling the DKFZ indel calling workflow 1.2.182-0 available from https://github.com/DKFZ-ODCF/IndelCallingWorkflow built on the platypus algorithm was used. This work-flow was most recently described by Wagener et al(3).

1. Kleinheinz KB, I.; Hubschmann, D.; Kensche, P.; Gu, Z.; Lopez, C.; Hummel, M.; Klapper, W.; Moller, P.; Inga, V.; Wagener, R. ACEseq – allele specific copy number estimation from whole genome sequencing. BioRxiv. 2017.
2. Popova T, Manie E, Rieunier G, Caux-Moncoutier V, Tirapo C, Dubois T, et al. Ploidy and large-scale genomic instability consistently identify basal-like breast carcinomas with BRCA1/2 inactivation. Cancer Res. 2012;72(21): 5454-62.
3. Wagener R, Seufert J, Raimondi F, Bens S, Kleinheinz K, Nagel I, et al. The mutational landscape of Burkitt-like lymphoma with 11q aberration is distinct from that of Burkitt lymphoma. Blood. 2019;133(9):962-6.

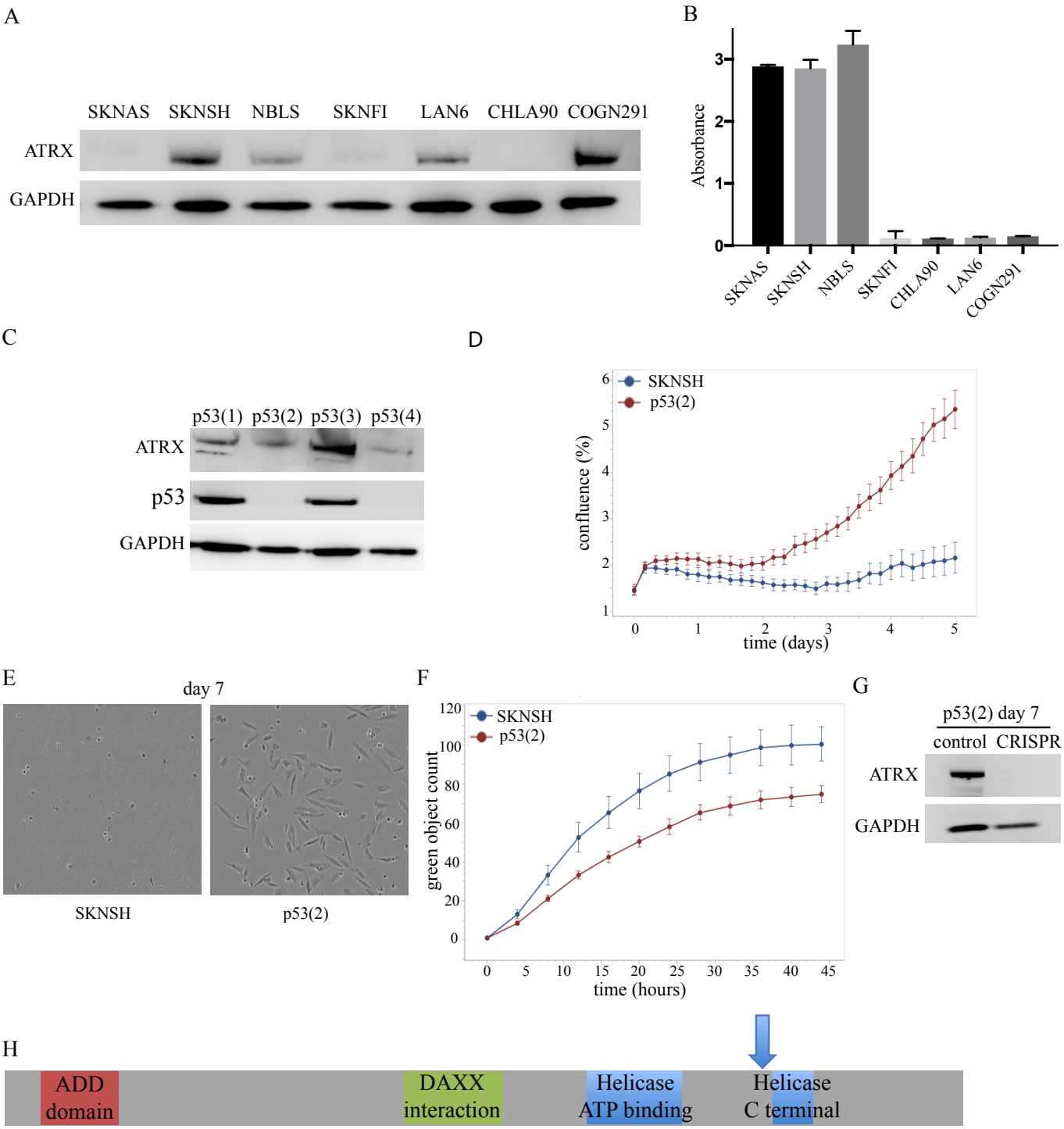

Fig S1: Generation of isogenic *ATRX* mutated neuroblastoma cell lines (A) ATRX expression by western blot in panel of *MYCN* non amplified neuroblastoma cell lines **(B)** Telomerase activity by TELOTAGGG Elisa **(C)** Western blot showing p53 expression in clones obtained after transfection with *TP53* CRISPR Cas9-GFP plasmid and single cell sorting of GFP positive cells. p53(1) and p53(2) were subsequently transfected with an *ATRX* CRISPR Cas9-RFP paprika plasmid and 2 x 96 well plates of RFP-paprika positive single cells sorted. It was only possible to generate *ATRX* deleted clones from the p53(2) cell line **(D)** Cell confluence quantified by the incucyte live cell analysis system following plating 2000 live, *ATRX* CRISPR Cas9-RFP paprika plasmid expressing cells per well in *TP53* wild type SKNSH and *TP53* deleted p53(2) cell lines **(E)** Representative bright field microscopy at day 7 **(F)** Quantitation of the number of cells giving a green fluorescent signal as a marker of apoptosis using the annexin V green assay (**G**) Western blot confirming absence of *ATRX* expression in surviving cells in the incucyte experiment **(H)** Diagram of the ATRX protein. The blue arrow indicates the position of the indels generated in *ATRX* in the three cell lines generated from p53(2): Clone A3 del pV1799-M1810fs. Clone E1: ins V1799-H1805fs. Clone E6 del pD1791-K1802fs.

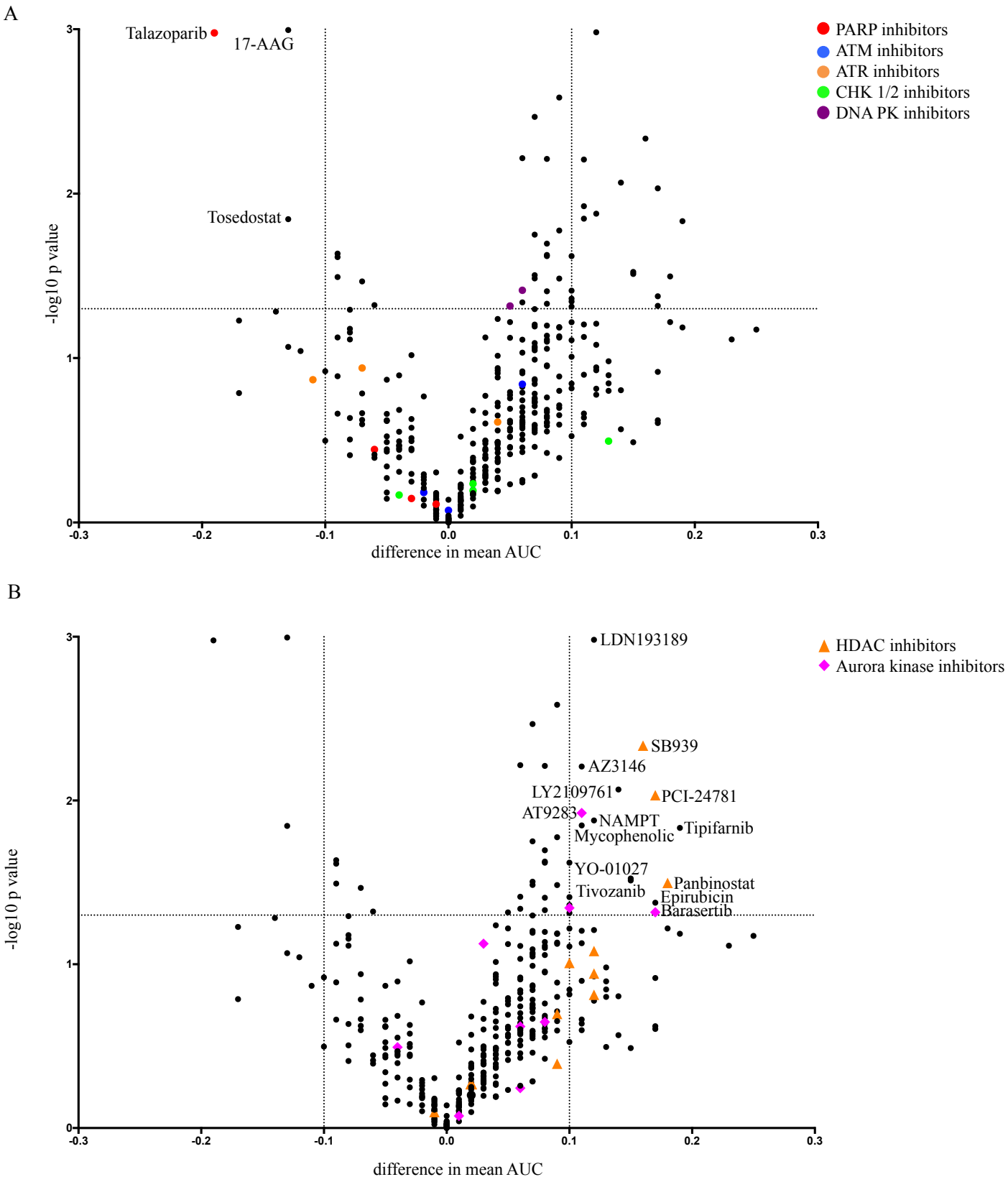

Figure S2: Therapeutic screening identifies specific vulnerabilities and patterns of resistance in *ATRX* mutant neuroblastoma. Volcano plots showing the difference in mean AUC and the negative log10 p-value of the difference in the AUC between the *ATRX* mutant and wild type groups for the 390 compounds tested in screen 1 **(A)** Compounds fulfilling the criteria for selective sensitivity in the *ATRX* mutants are highlighted in the top left quadrant. All inhibitors of the DNA damage response contained within the screen are colour coded according to the main mechanism of action **(B)** Compounds for which selective resistance was identified in the *ATRX* mutants are highlighted in the top right quadrant. For two classes of compounds: HDAC inhibitors and aurora kinase inhibitors, more than one compound from the same class was identified as showing selective resistance. All HDAC inhibitors and aurora kinase inhibitors contained in the screen are colour coded according to main mechanism of action

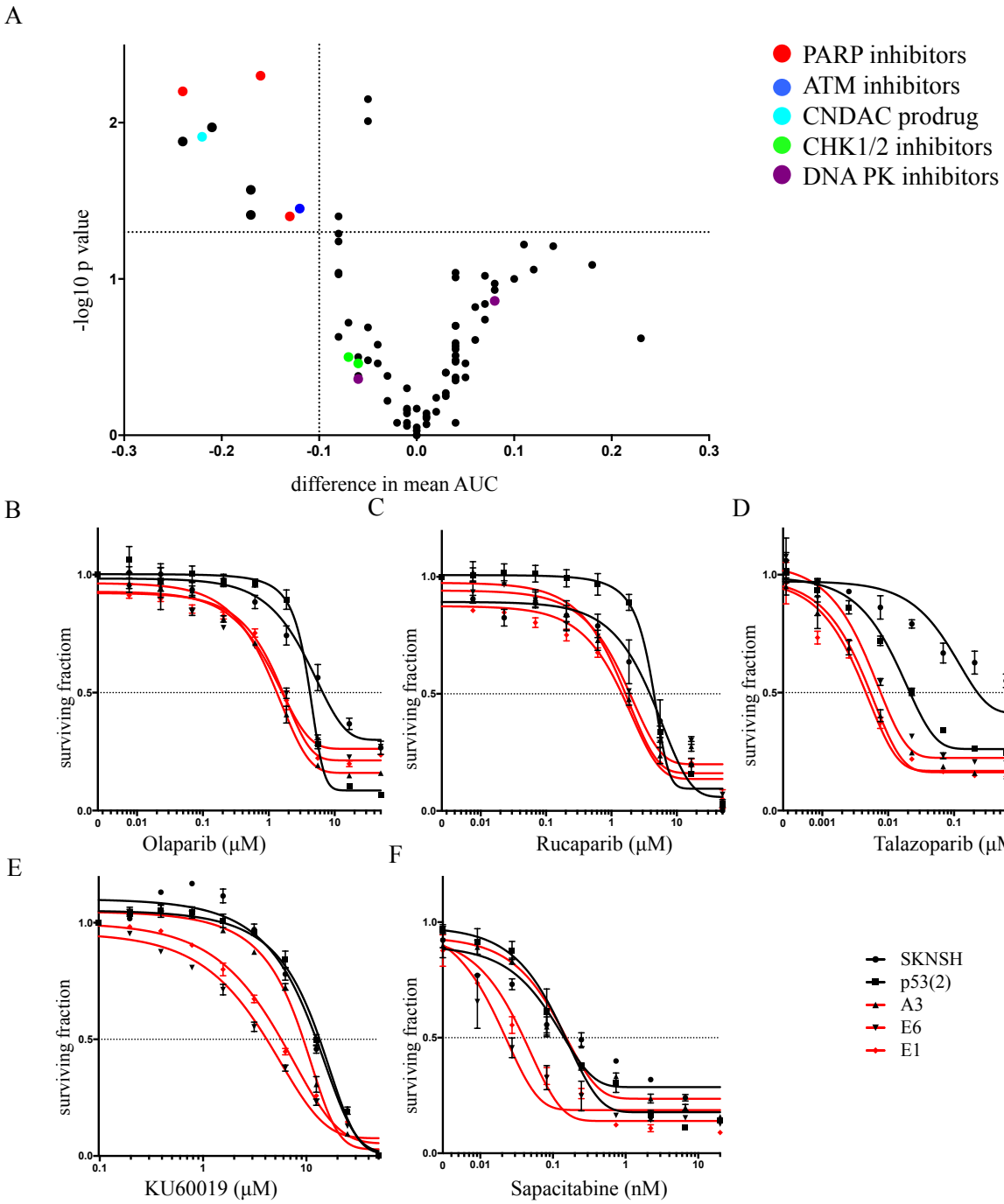

G

Mean SF_{50} (SD)	SKNSH	p53[2]	A3	E1	E6	*p-value (1)*	*p-value (2)*
Olaparib *(μM)*	6.9 (1.0)	4.4 (0.6)	2.1 (1.2)	2.5 (1.2)	2.5 (1.3)	*0.0004*	*0.01*
Rucaparib *(μM)*	3.9 (0.8)	3.9 (0.7)	1.6 (0.8)	1.8 (1.3)	2.2 (2.0)	*0.005*	*0.04*
Talazoparib *(nM)*	195.1 (113)	17.8 (3.9)	4.22 (1.8)	5.67 (2.2)	2.98 (1.6)	*0.0289*	*<0.0001*
Sapacitabine *(nM)*	186 (48)	215 (62)	109 (62)	38 (26)	68 (57)	*0.0004*	*0.0004*
KU60019 *(μM)*	11.4 (1.2)	13.1 (2.0)	9.5 (1.1)	4.7 (1.1)	5.6 (0.4)	*0.0002*	*0.0032*

Fig S3: Therapeutic screening identifies specific DNA damage repair pathway vulnerabilities in *ATRX* mutant neuroblastoma (A) Volcano plots showing the difference in mean AUC and the negative log10 p-value of the difference in the AUC between the *ATRX* mutant and wild type groups for the 80 compounds tested in screen 2. Inhibitors of the DNA damage response are colour coded according to the main mechanism of action **(B-D)** Representative dose response curves for the three PARP inhibitors identified as showing preferential sensitivity in the *ATRX* mutants in screen 2. **(E)** Representative dose response curve for KU60019 in isogenic panel of cell lines **(F)** Representative dose response curve for sapacitabine in isogenic panel of cell lines **(G)** Mean SF50 (surviving fraction50) for all compounds. Standard deviation represents results from 3 independent experiments. p-value(1) - comparison of both parent cell lines with ATRX mutants. p-value(2) - comparison of parent cell line (p53(2)) with ATRX mutants. All p-values indicated by 2 tailed unpaired students t test.

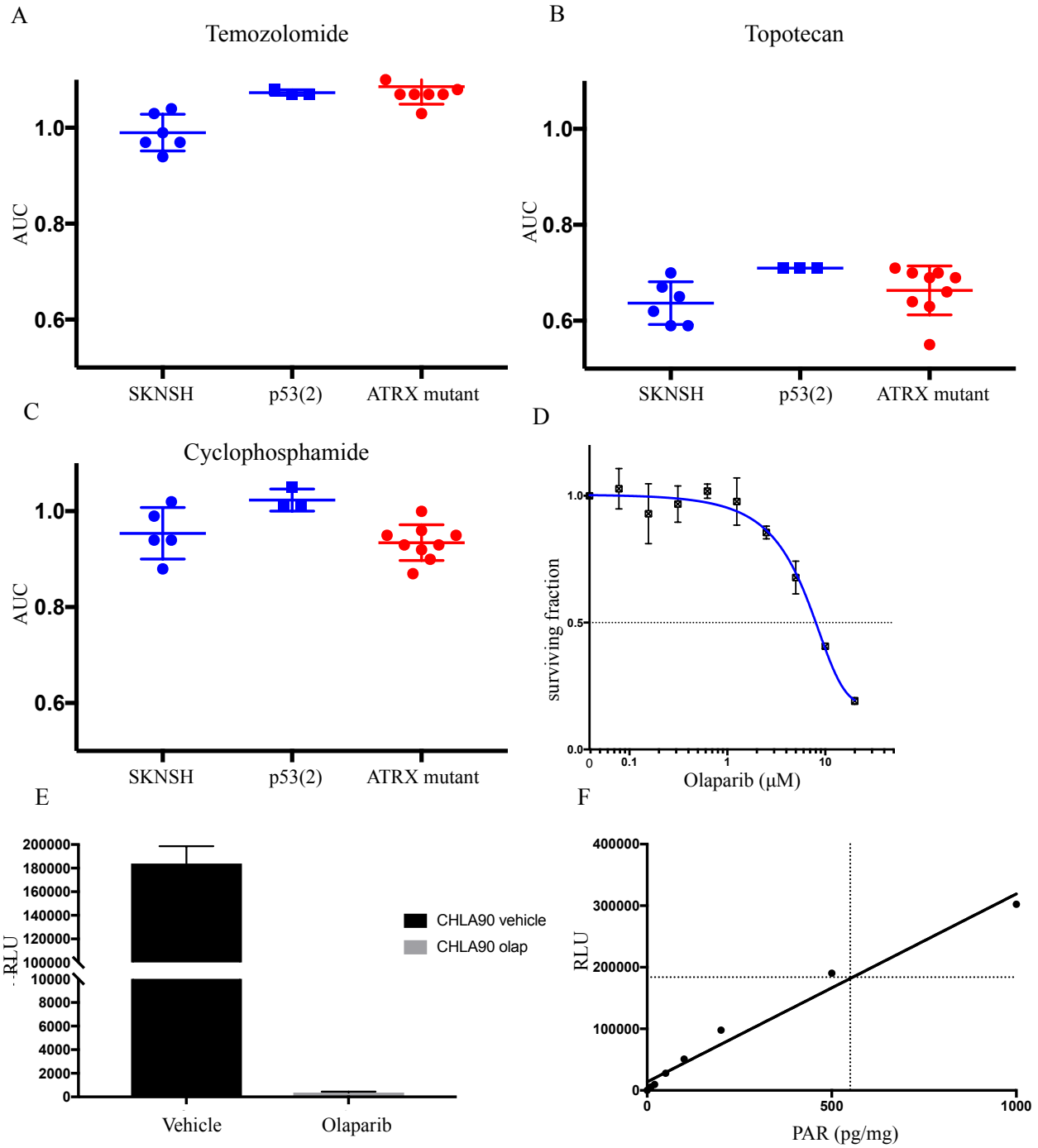

Figure S4: Comparison of chemo-sensitivity according to TP53 and ATRX status for **(A)** temozolomide **(B)** Topotecan and **(C)** cyclophosphamide, from compound screen data **(D)** Representative dose response curve for olaparib in CHLA90 cell line. Mean SF50 from 3 independent experiments 8.7μM (standard deviation 1.1). **(E)** PAR activity by HT PARP in vivo pharamcodynamic assay kits after treatment of CHLA90 cells with vehicle versus 1μM olaparib for 24 hours **(F)** PAR is quantified in pg/mg as a read out of relative light units (RLU).

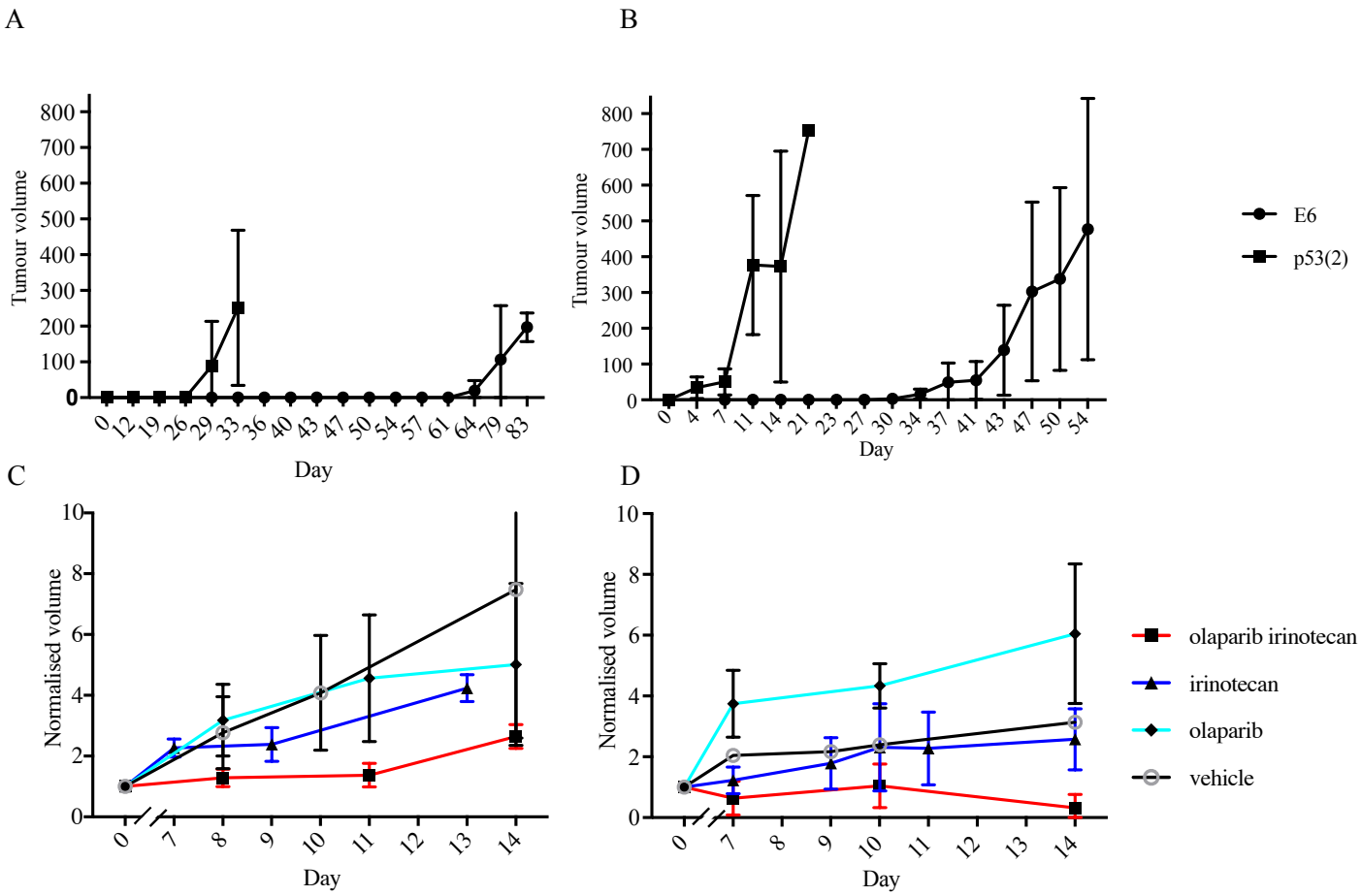

Figure S5: (A) Average tumour volume in cubic millimeters from the time of subcutaneous injection in passage zero E6 and p53(2) xenografts (**B**) Average tumour volume from the time of subcutaneous injection in passage 1 E6 and p53(2) xenografts **(C)** Normalised tumour volume curves for olaparib +/- irinotecan in p53(2) xenografts **(D)** Normalised tumour volume curves for olaparib +/- irinotecan in E6 xenografts

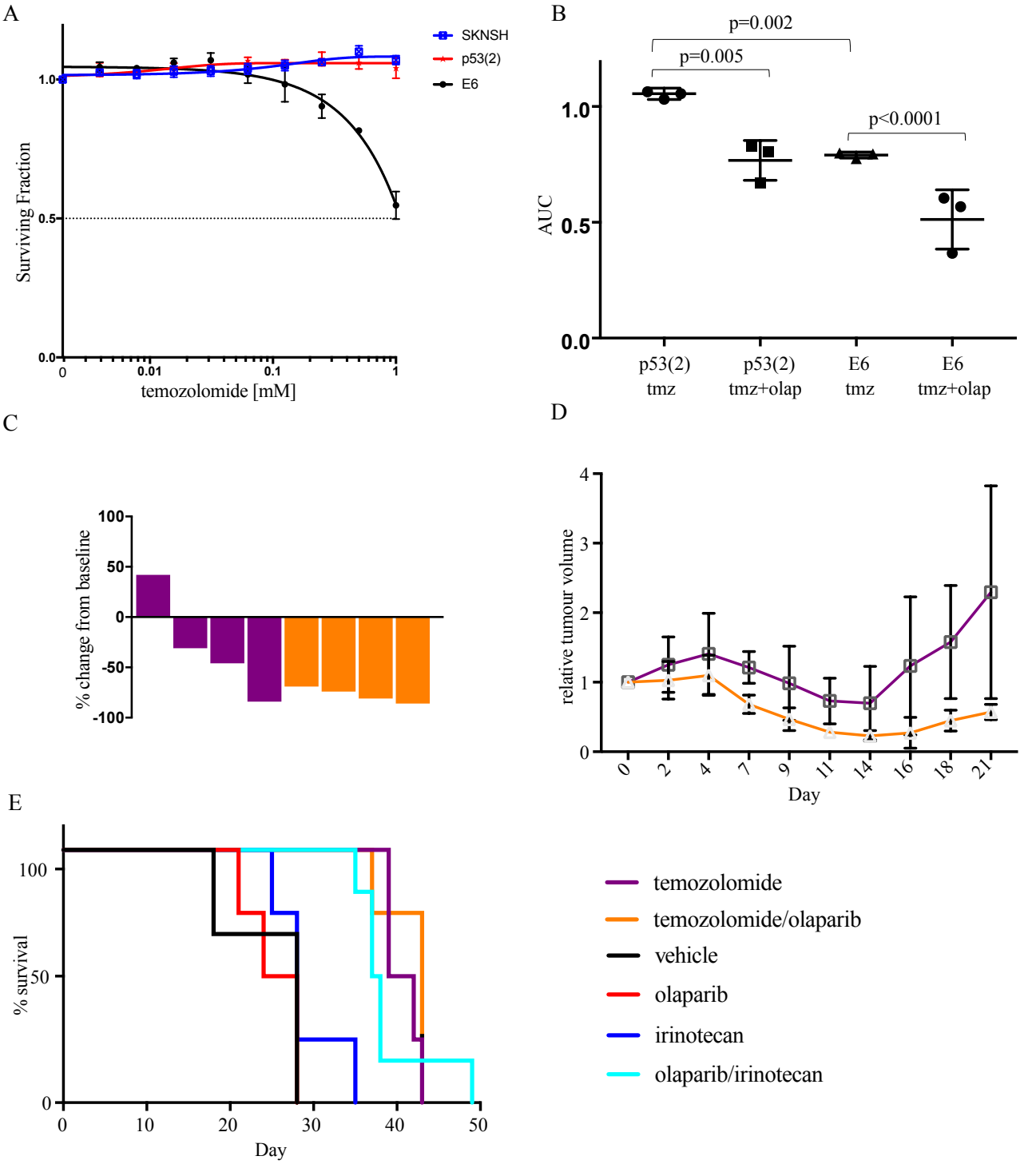

Figure S6: Preclinical evaluation of olaparib and temozolomide combination therapy (A) Representative dose response curve for temozolomide in isogenic cell line panel **(B)** Comparison of AUC results from 3 independent experiments for temozolomide alone (tmz) and temozolomide + 1uM olaparib (tmz+olap). p values by unpaired students t-test **(C)** Waterfall plot of day 14 response following single agent temozolomide and temozolomide/olaparib therapy in E6 xenografts **(D)** Tumour growth in E6 xenografts following treatment with temozolomide and temozolomide/olaparib combination therapy **(E)** Kaplan-Meier curve comparing survival of temozolomide containing treatment arms with irinotecan containing treatment arms in E6 xenograft